

Proceedings of the International Astronomical Union

Date of delivery: 5 May 2016

Journal and vol/article ref: IAU 1600036

Number of pages (not including this page): 6

This proof is sent to you on behalf of Cambridge University Press. Please check the proofs carefully. Make any corrections necessary on a hardcopy and answer queries on each page of the proofs

Please return the **marked proof** within **5** days of receipt to:

Managing editor of this symposium

Authors are strongly advised to read these proofs thoroughly because any errors missed may appear in the final published paper. This will be your ONLY chance to correct your proof. Once published, either online or in print, no further changes can be made.

To avoid delay from overseas, please send the proof by airmail or courier.

If you have **no corrections** to make, please email **managing editor** to save having to return your paper proof. If corrections are light, you can also send them by email, quoting both page and line number.

- The proof is sent to you for correction of typographical errors only. Revision of the substance of the text is not permitted, unless discussed with the editor of the journal. Only **one** set of corrections are permitted.
- Please answer carefully any author queries.
- Corrections which do NOT follow journal style will not be accepted.
- A new copy of a figure must be provided if correction of anything other than a typographical error introduced by the typesetter is required.

If you do not send any corrections to the editor within 5 days, we will assume your proof is acceptable.

- If you have problems with the file please contact

lwebb@cambridge.org

Please note that this pdf is for proof checking purposes only. It should not be distributed to third parties and may not represent the final published version.

Important: you must return any forms included with your proof. We cannot publish your article if you have not returned your signed copyright form.

NOTE - for further information about **Journals Production** please consult our **FAQs** at http://journals.cambridge.org/production_faqs

Author queries:

Typesetter queries:

Non-printed material:

Chapter 6: Particle acceleration and transport

Numerical RHD simulations of flaring chromosphere with *Flarix*

Petr Heinzel¹, Jana Kašparová¹, Michal Varady^{1,2}, Marian Karlický¹
and Zdeněk Moravec²

¹Astronomical Institute of the CAS, CZ-25165 Ondřejov, Czech Republic
email: petr.heinzel@asu.cas.cz

²J.E. Purkyně University, Physics Department, České mládeže 8, CZ-40096 Ústí nad Labem,
Czech Republic

Abstract. *Flarix* is a radiation–hydrodynamical (RHD) code for modeling of the response of the chromosphere to a beam bombardment during solar flares. It solves the set of hydrodynamic conservation equations coupled with NLTE equations of radiative transfer. The simulations are driven by high energy electron beams. We present results of the *Flarix* simulations of a flaring loop relevant to the problem of continuum radiation during flares. In particular we focus on properties of the hydrogen Balmer continuum which was recently detected by *IRIS*.

Keywords. Sun: flares, hydrodynamics, radiative transfer

1. Introduction

Recent advances in numerical RHD (radiation hydrodynamics) allow to solve complex problems of time evolution of the solar atmosphere affected by various flare processes (Allred *et al.* 2005, Kašparová *et al.* 2009, Varady *et al.* 2010, Allred *et al.* 2015). Resulting time-dependent atmospheric models (i.e. variations of the temperature, density, ionization and excitation of various species etc.) are then used as an input for synthesis of spectral lines and continua of atoms and ions under study. One of the ‘hot topics’ which attracts a substantial attention is the behavior of the so-called white light flares, and namely the problem of continuum formation. Recent finding of Heinzel & Kleint (2014) that the hydrogen Balmer continuum, previously rarely detected around the Balmer jump, can be easily seen in the flare spectra taken by *Interface Region Imaging Spectrograph IRIS* (De Pontieu *et al.* 2014) in the NUV channel represents a strong motivation for new numerical simulations. In this paper we first briefly describe the RHD technique on which our code *Flarix* is based and then use the flare simulations to predict the time behavior of the Balmer continuum. We then discuss the importance of the Balmer continuum for energy balance in the flaring chromosphere.

2. RHD code *Flarix*

The hybrid radiation–hydrodynamical code *Flarix* is based on three originally autonomous, now within *Flarix* fully integrated, codes: a test-particle (TP) code, a one-dimensional hydrodynamical (HD) code and time dependent NLTE radiative transfer code (for a detailed description of the code see Kašparová *et al.* (2009) and Varady *et al.* (2010)). *Flarix* is able to model several processes, which according to contemporary and generally accepted flare models occur concurrently in flares and play there important roles. The transport, scattering and progressive thermalization of the beam electrons

40 due to Coulomb collisions with particles of ambient plasma in the magnetized flaring
 41 atmosphere and the resulting flare heating corresponding to the local energy losses of
 42 beam electrons is calculated using an approach proposed by Bai (1982) and Karlický &
 43 Hénoux (1992) based on test particles and Monte Carlo method. This approach, fully
 44 equivalent to direct solution of the corresponding Fokker-Planck equation (MacKinnon
 45 & Craig 1991), provides a flexible way to model many various aspects of the beam
 46 electron interactions with the ambient plasma, converging magnetic field in the flare loop
 47 or with additional electric fields (Varady *et al.* 2014). These were proposed in various
 48 modifications of the standard CSHKP flare model (e.g. Turkmani *et al.* 2006, Brown
 49 *et al.* 2009, Gordovskyy & Browning 2012) or they can be related to the return current
 50 propagation (van den Oord 1990)). Owing to TP approach, the detailed distribution
 51 function of beam electrons is known at any instant and position along the flare loop.
 52 This information can be used to calculate a realistic distribution of HXR bremsstrahlung
 53 sources within the loop, their position size, spectra and directivity of emanating HXR
 54 emission (Moravec *et al.* 2013, Moravec *et al.* 2016).

55 Starting point of *Flarix* simulations are parameters of the non-thermal beam electrons.
 56 They are assumed to obey a single power law in energy, so their initial spectrum (in units
 57 of electrons $\text{cm}^{-2} \text{s}^{-1} \text{keV}^{-1}$) is

$$F(E, t) = \begin{cases} g(t)F(E) = g(t) (\delta - 2) \frac{F_{\text{max}}}{E_0^2} \left(\frac{E}{E_0}\right)^{-\delta} & , \text{ for } E_0 \leq E \leq E_1 \\ 0 & , \text{ for other } E . \end{cases} \quad (2.1)$$

58 The time dependent electron flux at the loop-top is determined by $g(t) \in \langle 0, 1 \rangle$, a function
 59 describing the time modulation of the beam flux, the maximum energy flux F_{max} , i.e.
 60 the energy flux of electrons with $E \geq E_0$ at $g(t) = 1$, the low and high-energy cutoffs
 61 E_0, E_1 , respectively, and the power-law index δ . These parameters can be derived either
 62 from observations like *RHESSI* (Lin *et al.* 2002) or set up arbitrarily. Another important
 63 parameter is the initial pitch angle distribution of non-thermal electrons $\Theta = \Theta(\vartheta_0)$. In
 64 case the function $\Theta(\vartheta_0)$ is normalized, the angle dependent initial electron flux is

$$F(E, \vartheta_0, t) = \Theta(\vartheta_0)F(E, t) . \quad (2.2)$$

65 The initial pitch angle distribution can be chosen by the user.

66 The 1D one fluid HD part of *Flarix* calculates the state and evolution of the plasma
 67 along semicircular magnetic field lines. The following set of equations is solved

$$\begin{aligned} \frac{\partial \rho}{\partial t} + \frac{\partial}{\partial s}(\rho u) &= 0 & \frac{\partial \rho u}{\partial t} + \frac{\partial}{\partial s}(\rho u^2) &= -\frac{\partial P}{\partial s} + F_g \\ \frac{\partial E}{\partial t} + \frac{\partial}{\partial s}(uE) &= -\frac{\partial}{\partial s}(uP) - \frac{\partial}{\partial s}\mathcal{F}_c + \mathcal{S} \end{aligned} \quad (2.3)$$

69 where s and u are the position and velocity of plasma along the fieldlines, respectively,
 70 and ρ is the plasma density. The gas pressure P , total plasma energy E , and the source
 71 term \mathcal{S} are

$$P = n_{\text{H}}(1 + x + \varepsilon)k_{\text{B}}T, \quad E = \frac{P}{\gamma - 1} + \frac{1}{2}\rho u^2, \quad \mathcal{S} = \mathcal{H} - \mathcal{R} + \mathcal{Q}, \quad (2.4)$$

72 where $\gamma = 5/3$ is the ratio of specific heats, k_{B} the Boltzmann constant, and T the
 73 temperature. The time-dependent hydrogen ionization x is provided by the NLTE code,
 74 ε accounts for the contribution from metals.

75 The terms on the right hand side of the system are: F_g the component of the gravity
 76 force in the parallel direction to the fieldlines, \mathcal{F}_c the heat flux calculated according to

the Spitzer classical formula, and \mathcal{S} includes all kinds of heating, i.e. mainly the total flare heating \mathcal{H} , the quiescent heating \mathcal{Q} assuring stability of the initial unperturbed atmosphere, and \mathcal{R} the radiative losses. The latter are computed in the NLTE part of the code by solving the time-dependent radiative-transfer problem in the bottom part of the flaring loop, for all relevant transitions of hydrogen, CaII and MgII (addition of helium losses is now in progress). In optically-thin regions of the transition region and corona the loss function of Rosner *et al.* (1978) is used.

Using the instant values of T , n_{H} , and beam electron energy deposit obtained by the HD and TP codes, time-dependent NLTE radiative transfer for hydrogen is solved in the lower parts of the loop in a 1D plan-parallel approximation. The hydrogen atom is approximated by a five level plus continuum atomic model. The level populations n_i are determined by the solution of the time-dependent system of equations of statistical equilibrium and charge and particle conservation equations

$$\frac{dn_i}{dt} = \sum_{j \neq i} n_j P_{ji} - n_i \sum_{j \neq i} P_{ij} \quad n_e = n_p + \varepsilon n_{\text{H}} \quad \sum_{j=1}^5 n_j + n_p = n_{\text{H}}, \quad (2.5)$$

where n_e and n_p are the electron and proton densities, respectively. P_{ij} contain sums of thermal and non-thermal collisional rates and radiative rates, the latter being pre-conditioned in the frame of MALI method (Rybicki & Hummer 1991). The NLTE part of *Flarix* gives a consistent solution for the non-equilibrium (time-dependent) hydrogen ionization.

3. Simulation of a short-duration electron beam heating

Here we present results of a simulation of the electron beam heating with a trapezoidal time modulation (see Fig. 1), $\delta = 3$, $E_0 = 20$ keV, $E_1 = 150$ keV, and $F_{\text{max}} = 4.5 \times 10^{10}$ erg cm⁻² s⁻¹ which represents a short beam-pulse heating with a moderate electron beam flux. As the initial unperturbed atmosphere we used the hydrostatic VAL-C atmospheric model of Vernazza *et al.* (1981) with a hydrostatic extension into the transition region and corona. Response of this atmosphere to the heating and the temporal evolution of the Balmer line emission is discussed in detail in Kašparová *et al.* (2009), see model H_TP_D3 there. In this particular RHD simulation, a simplified approach of Peres *et al.* (1982) was used to compute chromospheric radiative losses \mathcal{R} .

4. Hydrogen Balmer continuum

The time evolution of hydrogen atomic level populations, proton and electron densities and plasma temperatures has been used to synthesize the hydrogen Balmer continuum. For this purpose we have performed the formal solution of the transfer equation and obtained the time evolution of the Balmer continuum intensities. The results of *Flarix* simulations are shown in Fig. 2. The time evolution of temperature, primarily due to the electron beam heating, is shown in the top left panel. The time evolution of electron density consisting of the non-equilibrium contribution from hydrogen plus contribution from metals dominating around the temperature minimum region is shown in the top right panel. Around the height of 1000 km the electron density is substantially enhanced (reaching 10¹³ cm⁻³) which is typical for stronger flares. The bottom panel shows time evolution of the Balmer-continuum spectrum. The vertical dashed line is drawn at the wavelength 2830 Å which corresponds to the NUV spectral window of *IRIS* used by

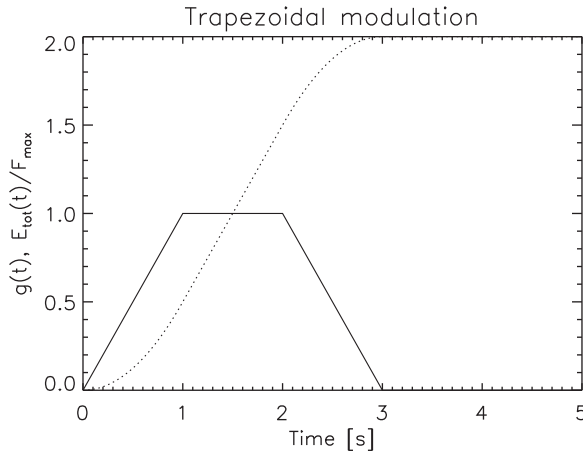


Figure 1. Time modulation $g(t)$ of the beam flux (solid line), dotted line denotes $\int_0^t g(t') dt' = E_{\text{tot}}(t)/F_{\text{max}}$. Total energy deposit is $E_{\text{tot}} = F_{\text{max}} \int_0^{t_1} g(t) dt$, where t_1 is the duration of the energy deposit. See also Eqs. (2.1).

118 Heinzel & Kleint (2014) to detect the Balmer continuum. The light curve at this particular
 119 wavelength is then shown in Fig. 3.

120 5. Discussion and conclusions

121 Our first *FlareX* simulations of time evolution of the hydrogen Balmer-continuum emis-
 122 sion are qualitatively consistent with the *IRIS* NUV light curves obtained by Heinzel &
 123 Kleint (2014) and Kleint *et al.* (2016). They show impulsive intensity rise followed by
 124 a gradual decrease. Rather slow non-equilibrium hydrogen recombination is perceptible
 125 in the light curve as expected but a more detailed analysis of this behavior is needed.
 126 However, for the present short trapezoidal electron-beam pulse lasting only a few seconds
 127 (Fig. 1), the synthetic intensity is lower in comparison with observations from Heinzel
 128 & Kleint (2014) or Kleint *et al.* (2016). This can be due to several reasons. First, the
 129 electron-beam flux used in this particular simulation is almost an order of magnitude
 130 lower than that derived from *RHESSI* spectra in Kleint *et al.* (2016). Second, the Balmer-
 131 continuum intensity was found to be increasing with the boundary pressure at $T=10^5$ K
 132 (see Table 1 in Kleint *et al.* (2016)) and the pressure in this simulation is low due to insuf-
 133 ficient evaporation. The beam duration is short and we may expect that a long-duration
 134 pulse or series of beam pulses will lead to stronger Balmer continuum, more consistent
 135 with the *IRIS* observations. Finally, for stronger beams one should not neglect the return
 136 currents which will modify the non-thermal hydrogen excitation and ionization (Karlický
 137 *et al.* 2004). Study of all these aspects is now in progress. We have also found that the
 138 chromospheric radiative cooling at the pulse maximum is dominated by the hydrogen
 139 subordinate continua and namely by the Balmer continuum – for static flare models this
 140 was already demonstrated by Avrett *et al.* (1986). Therefore, this continuum plays a
 141 critical role in the energy balance of the flaring chromosphere, the site where most of
 142 the electron-beam energy is deposited. Since the Balmer continuum is mostly optically
 143 thin in the flaring chromosphere, the total radiative losses integrated along the relevant
 144 formation heights are directly related to the observed Balmer-continuum spectral inten-
 145 sity. The *IRIS* observations thus provide an extremely important constraint on the flare
 146 energetics. Moreover, accepting the idea of backwarming of the flare photosphere, one

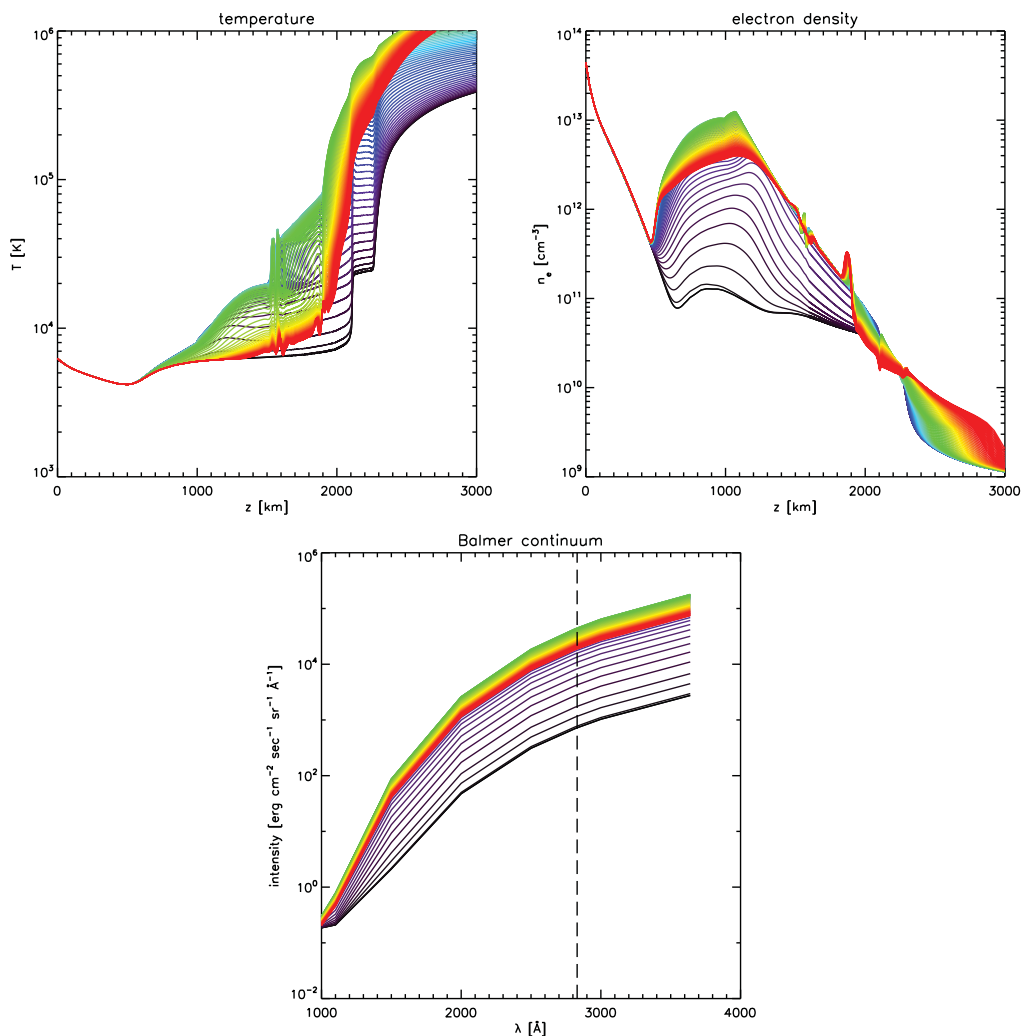


Figure 2. Results of *Flarix* simulations for the trapezoidal electron beam pulse described in Section 3. The three panels show, respectively, the time evolution of temperature (top left), electron density (top right), and the hydrogen Balmer-continuum spectrum (bottom). In the latter panel we indicate the wavelength used by *IRIS* to detect this continuum (see the vertical dashed line). The gray-scale coding represents the time evolution from initial stages (black) through the flare maximum (light gray) up to the end of simulation (dark gray). In the online version of the paper the time evolution is color coded – for increasing time the colors change from black to blue-green-yellow-red.

147 gets directly the amount of radiative energy which should heat the lower atmospheric
 148 layers. This issue is discussed in Kleint *et al.* (2016) using the *IRIS* and optical/infrared
 149 continuum observations. We conclude that the *Flarix* simulations coupled to broad-band
 150 continuum observations should provide a clue to the long-lasting mystery of the white-light
 151 flares.

152 This project was supported by the EC Program FP7/2007-2013 under the F-CHROMA
 153 agreement No. 606862 and by the grant P209/12/0103 of the Czech Funding Agency
 154 (GACR).

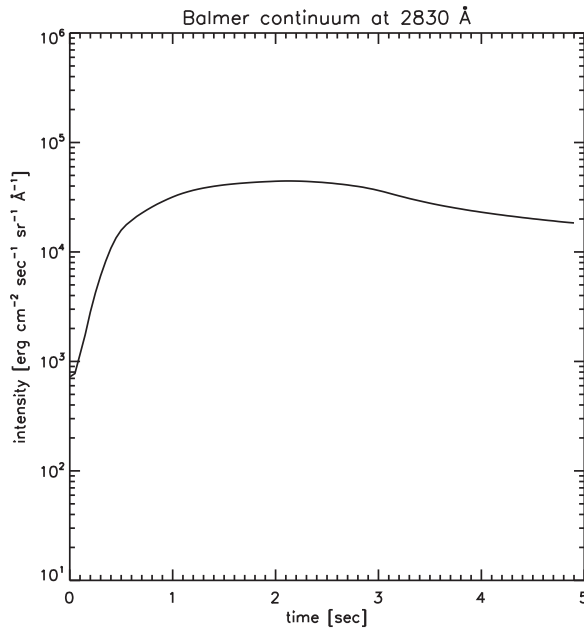


Figure 3. Simulated time evolution (light-curve) of the hydrogen Balmer continuum intensity at the wavelength selected for *IRIS* detection in the NUV channel (dashed vertical line in Fig. 2).

155

References

- 156 Allred, J. C., Kowalski, A. F., & Abbett, Carlsson, M. 2015, *ApJ*, 809, 104
 157 Allred, J. C., Hawley, S. L., Abbett, W. P., & Carlsson, M. 2005, *ApJ*, 630, 573
 158 Avrett, E. H., Machado, M. E., & Kurucz, R. L. 1986, in *The lower atmosphere of solar flares*,
 159 ed. D.F. Neidig, Sunspot (NSO), New Mexico, 216
 160 Bai, T. 1982, *ApJ*, 259, 341
 161 Brown, J. C., Turkmani, R., Kontar, E. P., MacKinnon, A. L., & Vlahos, L. 2009, *A&A*, 508,
 162 993
 163 De Pontieu, B., Title, A. M., Lemen, J. R., *et al.* 2014, *Sol. Phys.*, 289, 2733
 164 Gordovskyy, M. & Browning, P. K. 2012, *Sol. Phys.*, 277, 299
 165 Heinzel, P. & Kleint, L. 2014, *ApJ*, 794:L23
 166 Karlický, M. & Hénoux, J. C. 1992, *A&A*, 264, 679
 167 Karlický, M., Kašparová, J., & Heinzel, P. 2004, *A&A*, 416, L13
 168 Kašparová, J., Varady, M., Heinzel, P., Karlický, M., & Moravec, Z. 2009, *A&A*, 499, 923
 169 Kleint, L., Heinzel, P., Judge, P., & Krucker, S. 2016, *ApJ*, in press (arXiv:1511.04161v1)
 170 Lin, R. P., Dennis, B. R., Hurford, G. J., *et al.* 2002, *Sol. Phys.*, 210, 3
 171 MacKinnon, A. L. & Craig, I. J. D.. 1991, *A&A*, 251, 693
 172 Moravec, Z., Varady, M., Karlický, M., & Kašparová, J. 2013, *Central European Astrophys.*
 173 *Bull.*, 37, 535
 174 Moravec, Z., Varady, M., Kašparová, J., & Kramoliš, D., 2016, *AN*, in press
 175 van den Oord, G. H. J.. 1990, *A&A*, 234, 496
 176 Peres, G., Serio, S., Vaiana, G. S., & Rosner, R. 1982, *ApJ*, 252, 791
 177 Rybicki, G. B. & Hummer, D. G. 1991, *ApJ*, 245, 171
 178 Rosner, R., Tucker, W. H., & Vaiana, G. S. 1978, *ApJ*, 220, 643
 179 Turkmani, R., Cargill, P. J., Galsgaard, K., Vlahos, L., & Isliker, H. 2006, *A&A*, 449, 749
 180 Varady, M., Kašparová, J., Moravec, Z., Heinzel, P., & Karlický, M. 2010, in *IEEE Transactions*
 181 *on Plasma Science*, 38, 2249
 182 Varady, M., Karlický, M., Moravec, Z., & Kašparová, J. 2014, *A&A*, 563, A51
 183 Vernazza, J. E., Avrett, E. H., & Loeser, R. 1981, *ApJS*, 45, 635